Diurnal Variations in Summer Monsoon Precipitation over Thailand and Its Vicinity Observed from Ten Years of TRMM Data

Atsamon Limsakul[1,*], Usa Humphries[2], Angkool Wangwongchai[2], Thanet Chitsuphaphan[2] and Prungchan Wongwises[3,4]

[1]Environmental Research and Training Center, Technopolis, Klong5, Klong Luang, Pathumthani 12120 Thailand
[2]Department of Mathematics, King Mongkut's University of Technology Thonburi, Bang Mod, Thung Khru, Bangkok 10140 Thailand
[3]The Joint Graduate School of Energy and Environment, King Mongkut's University of Technology Thonburi,
Bang Mod, Thung Khru, Bangkok 10140 Thailand
[4]Center of Excellence on Energy Technology and Environment, Ministry of Education, Thailand
*Corresponding author: atsamon@deqp.go.th
Tel.: 66-2-577-1136-7; Fax: 66-2-577-1138

Abstract: On the basis of Empirical Orthogonal Function (EOF) and harmonic analysis, spatial patterns of diurnal cycles of precipitation during a rainy season over Thailand and its vicinity were examined using 3-hourly, 0.25° TRMM data for the time period 2000-2009. Results revealed that the leading two EOFs and harmonics could explain most of diurnal precipitation variations. The first EOF and harmonic represent the diurnal cycle with an afternoon-evening peak and amplitude of 30-88% of the climatological mean. This dominant feature reflects land-sea difference in the atmospheric response to solar radiation forcing, representing potential instability forced by the surface heat flux, insolation and long-wave radiative cooling during the day and night. Whereas, the second EOF and harmonic denote the semidiurnal cycle, with nocturnal and early morning maxima and amplitude of 10-33% of the climatological mean. The secondary sub-daily cycle represents a complementary local variation, and is associated with mesoscale dynamics of convective systems and its interactions with local thermally induced circulations. The findings from this study provide evidence to broaden the understanding of local climate, and to validate certain parameterizations in numerical models as well as to improve weather forecast accuracy. However, further analysis should relate and simulate the identified diurnal variations to large-scale atmospheric circulation modes . This future work may lead to better understand the mechanisms of diurnal precipitation variations under a recent widening of the tropical belt and an anthropogenically warmed climate.

Keywords: Diurnal variation, Precipitation, Empirical Orthogonal Function, Harmonic, Thailand.

1. Introduction

Diurnal precipitation variations are the most basic dynamics of climate system especially over the tropics. It is often related to physical processes governed by the atmosphere-ocean-land-cryosphere system's response to solar forcing, and is connected with local and regional atmospheric circulation and/or dynamics [1-5]. Study on the diurnal cycle of precipitation is therefore helpful to enhance the understanding of local climate, and to validate and improve the fundamental physical processes in the regional climate models. This is why diurnal variations in precipitation have been extensively analyzed for several decades [2-3, 6-10]. The earlier studies primarily used hourly station data which were available only in some regions with good maintained networks of long systematic records [1-2, 10-11]. This has resulted in most of the studies in the earlier part of the twentieth century concentrated in the western hemisphere [1, 12]. With the recent advances in the satellite remote-sensing techniques of precipitation estimation at improved accuracy and spatial/temporal resolutions, however, there has been an increasing number of studies in the last two decades, focusing on the diurnal patterns in the relatively less explored regions of the world [2-3, 5, 10, 13-14].

In the past several years, a number of quasi-global high-resolution satellite products have been developed to produce near real-time hourly or 3-hourly precipitation at 0.25° or better resolution for the entire tropics and middle latitudes [15-18]. The Tropical Rainfall Measuring Mission (TRMM) satellite launched in 1997, for example, provides such data by using a unique combination of instruments designed purely for precipitation observation [19-20]. More than a decade since the launch of the TRMM, a series of high-resolution, quasi-global, near-real-time, TRMM-based precipitation estimates has been available (http://mirador.gsfc.nasa.gov/) to scientists to make use for

analyzing and revealing much more details of diurnal variations over global tropics. These studies include Sorooshian et al. (2002), Nesbitt and Zipser (2003), Yang and Smith (2006), Dai et al. (2007), Hirose et al. (2008), Kikuchi and Wang (2008) and Takahashi et al. (2010) [2-3, 5, 10, 13-14, 21] who conducted detailed regional/global level analyses across the entire earth surface. On the basis of these satellite observations, it has been shown that maximum precipitation tends to occur in the late afternoon/early evening over land and in the early morning over ocean, and amplitude of the diurnal cycle over land is much larger than that over ocean.

In this study, the diurnal cycle of precipitation was analyzed for Thailand where the diurnal precipitation patterns and associated high-frequency climate variability are still less explored. The present analysis was limited to a rainy season (June to September), which a majority of precipitation is driven primarily by the Asian summer monsoon. The results of this study would help to better understand the role of local-level processes on the amount and frequency of precipitation events, and potentially further enhance short-term weather forecasting. It would also help in further understanding other related processes including rates of evaporation and increased efficiency of agricultural irrigation activities.
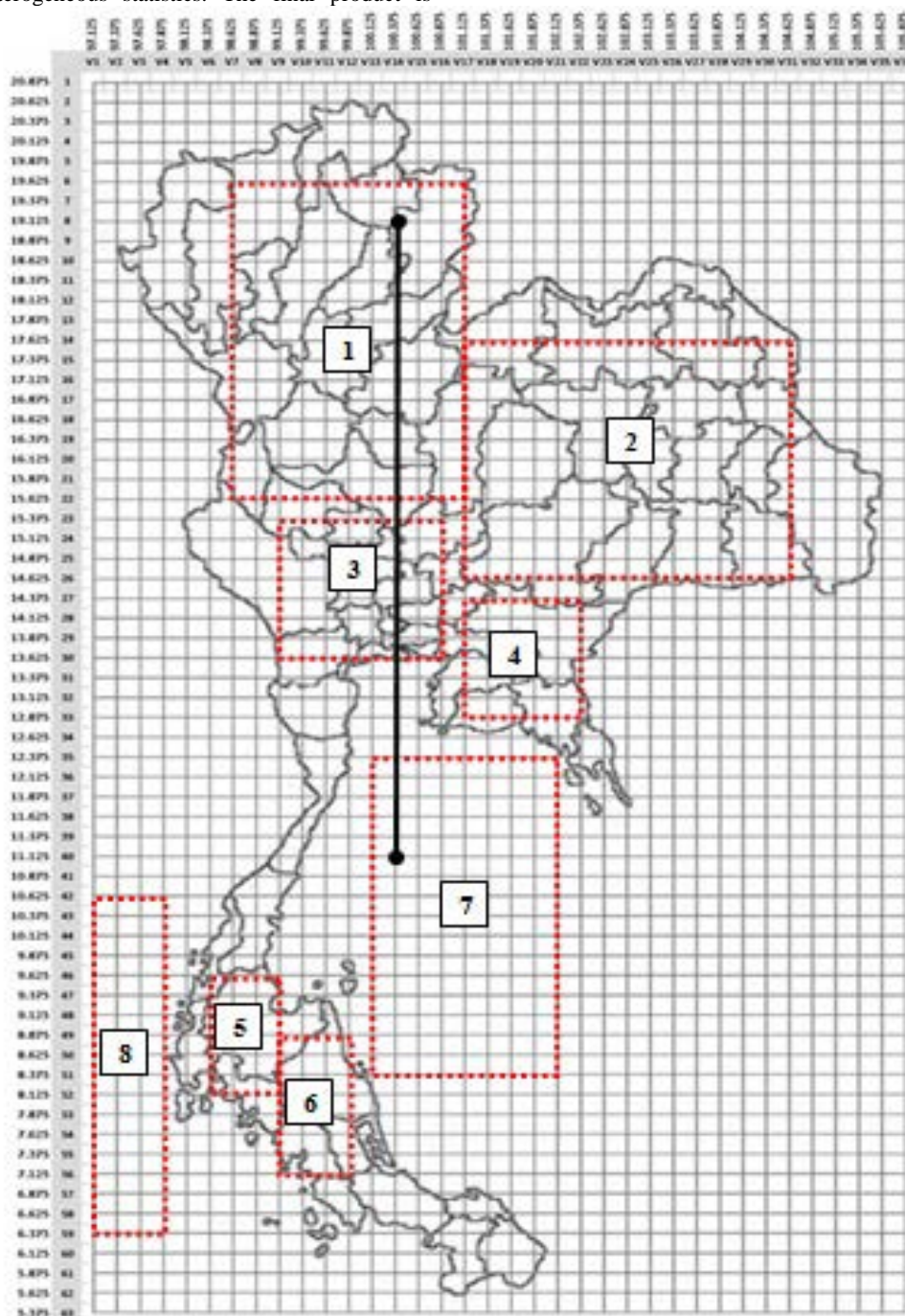
2. Experimental

2.1 TRMM data and quality control check

The TRMM 3B42 version 6 of high-resolution (0.25° X 0.25° and 3 hourly) precipitation data for 10-year period (2000-2009) was used. The data set is produced on the basis of TRMM Multi-satellite Precipitation Analysis (TMPA), which provides a calibration-based sequential scheme for combining precipitation estimates from multiple satellites and gauge analyzes where feasible at fine scales [18]. The goal of TMPA is to provide the "best" estimate of precipitation in each grid box at each observation

time. The TMPA estimates are produced in four stages: 1) precipitation-related microwave data collected by the Microwave Imager (TMI), the Special Sensor Microwave Imager (SSM/I), the Advanced Microwave Scanning Radiometer-Earth Observing System (AMSR-E), and the Advanced Microwave Sounding Unit B (AMSU-B) are calibrated and combined, 2) the infrared (IR) data collected by the international constellation of geosynchronous earth orbit (GEO) are created using the calibrated microwave precipitation, 3) the microwave and IR estimated are then combined, and 4) rain gauge data are finally incorporated. A simple approach is applied to combine the microwave and IR estimates, namely, the physically based combined microwave estimate are taken 'as is' where available, and the remaining grid boxes are filled with microwave-calibrated IR estimates [18]. This scheme provides the "best" local estimate at the expense of a time series that contains heterogeneous statistics. The final product is obtained by rescaling it in reference to rain gauge data on a monthly time scale.

The data during a rainy season (June to September) for the period 2000-2009 for our study domain which covers the entire Thailand and it vicinity (5.375-20.875° latitude, 97.125-105.875° longitude) (Figure 1) were extracted from TRMM 3B42 V6. Although quality control (QC) for TRMM data has been regularly done by the TRMM Science Data and Information System (TSDIS), we decided to recheck the QC of the extracted TRMM data to ensure for their completeness and reliability. The simple QC procedures applied in this study included: (1) checking any obviously erroneous data and missing values; (2) calculating climatological maximum and mean values and standard deviations for each grid of the data; and (3) examining outliers on the basis of the data distribution.

Figure 1. The boundary and gridded boxes of the extracted TRMM 3B42 version 6 for the study domain which covers the entire Thailand and its vicinity during a rainy season (June to September) for the period 2000-2009.

2.2 Diurnal cycle analysis

To reconstruct the diurnal cycle of precipitation with sufficient sampling, multi-year composites of TRMM's precipitation estimates were prepared. This is due to the fact that each overpass of a given location by TRMM's narrow (215 km) swath occurs infrequently (~0.5–2 times day^{-1}), leading to reduction in temporal sampling when compared to IR satellite measurement or hourly surface observations [13]. Local solar time (LST), instead of coordinated universal time (UTC) was used to facilitate comparison of diurnal cycles among all grids and to give a clearer picture of diurnal distribution of precipitation. UTC was converted to LST based on the longitudinal distance between each grid and 0° [2-3]. The piece-wise cubic hermite polynomial interpolation was then applied to obtain the LST precipitation at given times (0000, 0300, 0600, 0900, 1200, 1500, 1800 and 2100 LST) and at each grid point, so that data at each grid point represent its local time [22].

As one of the extensive methods used in investigating diurnal variations [4, 6, 11-12, 23-24], a harmonic analysis of multi-year averaged, composite 3-hourly TRMM precipitation data at each grid box was carried out to estimate the amplitude and phase of diurnal (24 h, S1), semidiurnal (12 h, S2) and other high frequency cycles to precipitation variations. The basic form of a harmonic equations is

$$P = \overline{P} + \sum_{r=1}^{N/2} A_r cos(r\theta - \varphi_r), \qquad (1)$$

where the estimated precipitation frequency is P; θ is derived as $2\pi X/N$ with X as the hour and N is the number of observation, i.e. 24. ϕ_r is the phase angle of the harmonic curve, also reinterpreted as the time of maximum precipitation. $\overline{P}$ is the average 3-hourly frequency over the N observations, and r is the frequency or number of times which the harmonic curves is repeated in 24 h. The standardized amplitude that mainly reveals the relative importance of a diurnal cycle at each grid box is calculated by $A_r / 2\overline{P}$. The portion of variance explained is computed as $V_r = A_r^2 / 2\sigma^2$, with σ as the standard deviation of the 24 h. precipitation frequency values.

To reveal the unified feature and dominant modes of the diurnal cycle over the entire study area, climatological composite 3-hourly data of all extracted grid boxes were further analyzed by the Empirical Orthogonal Function (EOF) method. The EOF also known as Principal Component Analysis (PCA) is descriptive multivariate statistical method [25-28]. It is based on a linear transformation to decompose a space-time field into orthogonal basis function (eigenvalue/eigenvector), while retaining as much as possible of the variance presented in the original data sets. The EOF analysis is capable of capturing both stationary oscillations such as the Arctic Oscillation (AO) [29] and transient oscillations such as the Madden–Julian oscillation (MJO) [30]. The major aim of EOFs is to achieve a decomposition of a discrete and continuous space-time field X (t, s), where t and s denote respectively time and spatial position, as

$$X(t,s) = \sum_{k=1}^{M} c_k(t)u_k(s), \qquad (2)$$

where M is the number of modes contained in the field, using an optimal set of basis functions of space (s) and expansion functions of time $c_k(t)$. In practice, the EOF technique aims at finding a new set of variables that capture most of the observed variance from the data through linear combinations of the original variables. Kikuchi & Wang (2008) [3] employed this

method to describe diurnal variation of the global tropical precipitation. More recently, Teo et al. (2011) [31] used the EOF to diagnose the dynamics and physics of observed and modeled diurnal rainfall in the Maritime Continent.
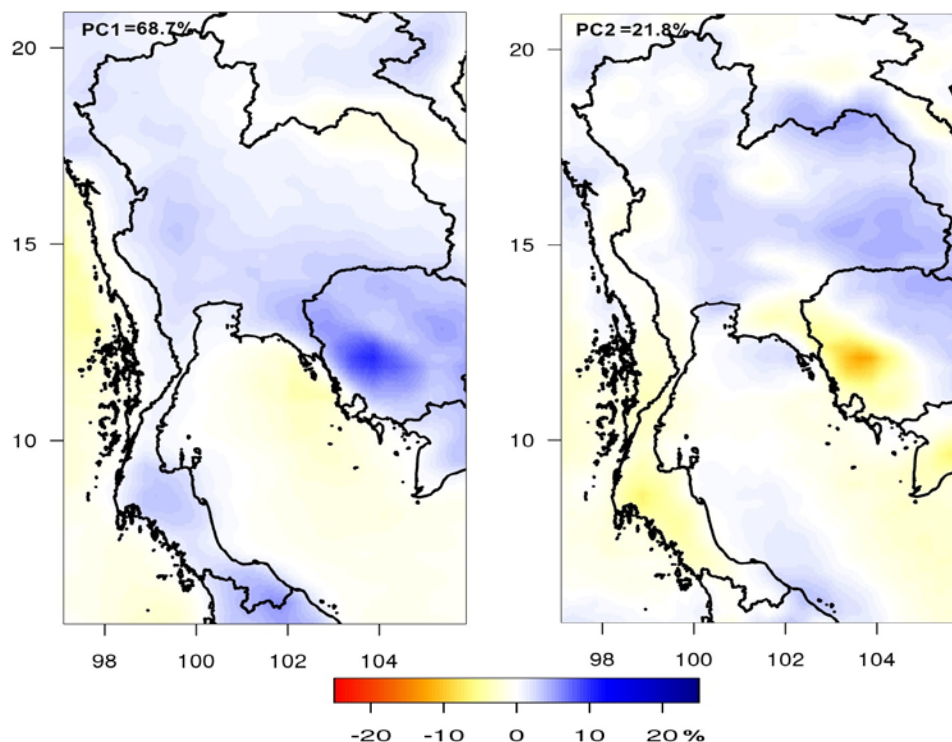
3. Results and discussion
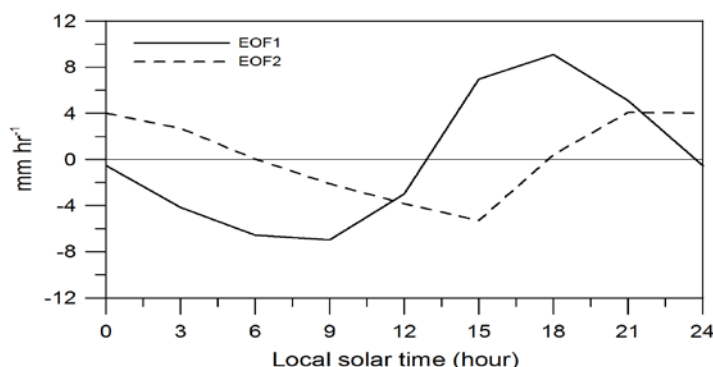
3.1 Quality of the extracted TRMM data

The QC examination revealed that the extracted TRMM data for our study domain during a rainy season for the period 2000-2009 were relatively good quality compared to other 3-hourly and daily station data being used in Thailand for climate study. There were only 0.026% of missing values in which were detected in 2001, 2003 and 2004, respectively. No extreme outliers were found. It should be noted that averaged and maximum values of TRMM data extracted for the study domain were comparable ranges of the Indochina and global regions used by Takahashi et al. (2010) [5] and Kikuchi and Wang (2008) [3]. Comparison of TRMM 3B42 V6 with daily rainfall data collected from more than 100 gauges in Thailand during 1993-2002, Chokngamwong and Chiu (2008) [32] found that the TRMM data set has been improved significantly with bias, root-mean-square difference (RMSD) and mean absolute difference (MAD) of only -0.12, 11.89 and 5.02 mm day^{-1}, respectively. Based on quality checking, such very low percentages of missing values did not substantially affect further analyzes of spatio-temporal patterns of diurnal precipitation variations. We then decided to simply neglect the missing data in the following calculations and statistical analysis, which means that the long-term means were used to replace the missing data.

3.2 Dominant spatio-temporal patterns of diurnal precipitation variations over Thailand and its vicinity

Figures 2 and 3 show the results of EOF analysis based on climatological 3-hourly averages of TRMM precipitation data during a rainy season for the period 2000-2009. The first two modes alone can account for 68.7% and 21.8% of the total variance, respectively (Figure 2). These two modes represent dominant diurnal precipitation patterns which all together can explain 90.5% of the total variance in the extracted TRMM 3B42 V6 over the study domain. The corresponding principal component coefficient series of the two leading EOFs, namely EOF1 and EOF2, both have dominant diurnal periodicity (Figure 3). EOF1 captures about three times more variance than EOF2, and represents the fundamental land-sea contrast of diurnal precipitation cycles, with opposite signs observed for the land (positive values) and coastal sea (negative values) (Figure 2). It reflects the difference between land and sea in the atmospheric response to solar radiation forcing during the period of intensive convective activity associated with the strengthening of Asian summer monsoon [3]. It basically represents the rise and fall of potential instability forced by the surface heat flux, insolation and long-wave radiative cooling during the day and night [31]. EOF1 also illustrates more intense diurnal precipitation cycle over the high terrain and a mountain range over a basin-shape plain around Tonle Sap Lake in Cambodia (Figure 2). It is possibly due to the combined effect of land-lake circulation over and around the Tonle Sap Lake [5], and stronger solar forcing on the mountain slopes as well as valley breeze convergence towards the mountain ridges [33]. Another noteworthy characteristics of diurnal precipitation cycle as captured by EOF1 is that precipitation maximum tends to occur in the late afternoon (1500-1800 LST) over land areas and in the early morning (0600–0900 LST) over coastal seas in the vicinity of land and peninsula (Figure 3).

Figure 2. Spatial structures in form of eigenvectors of EOF1 and EOF2 for 3-hourly climatological means of TRMM precipitation data during a rainy season for the period 2000-2009.

Figure 3. The corresponding principal component coefficient series of EOF1 and EOF2 for 3-hourly climatological means of TRMM precipitation data during a rainy season for the period 2000-2009.

Positive (negative) spatial loadings in the central and northeast (east and south) illustrated by EOF2 denote a complementary local variation, which is a component deviating from the fundamental diurnal cycle that is expressed by EOF1. It is usually associated with intrinsic mesoscale dynamics of convective systems and its interactions with gravity waves, density currents and local thermally induced circulations in coastal sea or mountainous terrain [31]. The sub-daily feature of EOF2 can be characterized as mid-night peak in the central and northeast of Thailand whereas as afternoon peak in the east and south as well as some parts of Cambodia and Gulf of Thailand (Figure 3).

3.3 Sub-daily harmonic cycles of precipitation amount over the selected areas

In this section, the results from harmonic analysis were further presented to provide more detailed information on sub-daily precipitation variations in terms of variance, amplitude and phase at each grid box. For comparative purpose of spatial coherences and differences, the diurnal (24 h, S1), semidiurnal (12 h, S2) and other high frequency cycles to the diurnal variation of precipitation and corresponding harmonic parameters were averaged for 8 selected areas (Figure 1). These areas represent different characteristics of climate and geography which includes main land, low-lying plain, peninsula and costal area/seas. The multi-year mean anomalies of 3-hourly precipitation amount during a rainy season, and sub-daily variations estimated by the first four harmonics for each selected areas are shown in Figures 4 and 5. While harmonic parameters in terms of variance, amplitude and phase of diurnal variations estimated from the first and second harmonics in which each parameter was averaged from each selected areas are summarized in Tables 1 and 2. On the basis of the harmonic analysis of 8 selected areas, distinctive features of sub-daily precipitation variations in terms of diurnal amplitude and phase were observed especially over land area and costal sea (Figures 4 and 5). For a rainy season, the first harmonic (24-h predominating cycle) dominates the sub-daily precipitation variations of all selected areas (Figures 4 and 5), and accounts for most of its diurnal variance (Table 1). However, there is a secondary 12-h semidiurnal oscillation which explains the remaining variance ranging from 7.1 to 26.5% (Table 2). Based on the variance explained the strength of individual harmonic fitting order, it is indicated that sub-daily precipitation variations of all selected areas can be reproduced perfectly by the first four harmonics (Figures 4 and 5).

Table 1. Mean first harmonic parameters of sub-daily precipitation variations.
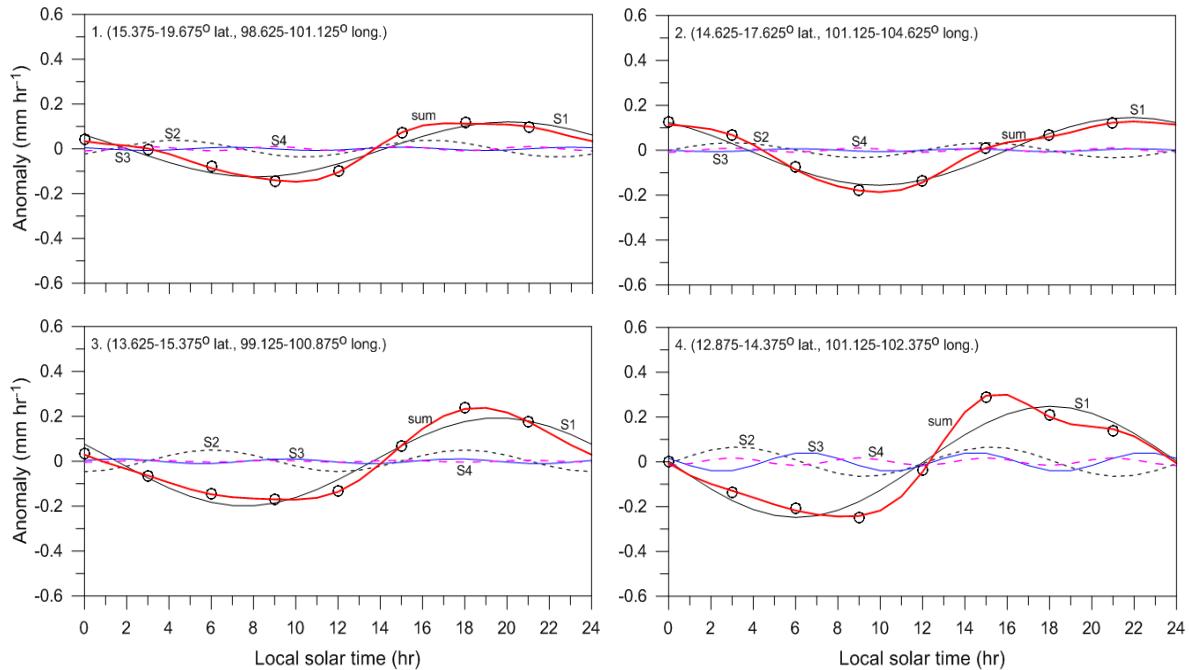
Area	Variance (%)	Amplitude* (%)	Phase (LST)
1	82.0	51.3	19.46
2	84.0	56.5	18.42
3	91.6	87.6	19.31
4	87.2	76.4	18.08
5	70.2	61.2	14.59
6	76.9	69.9	15.45
7	69.2	39.7	05.30
8	84.7	29.7	08.26

*percentage relative to 3-hourly means of precipitation during a rainy season for the period 2000-2009
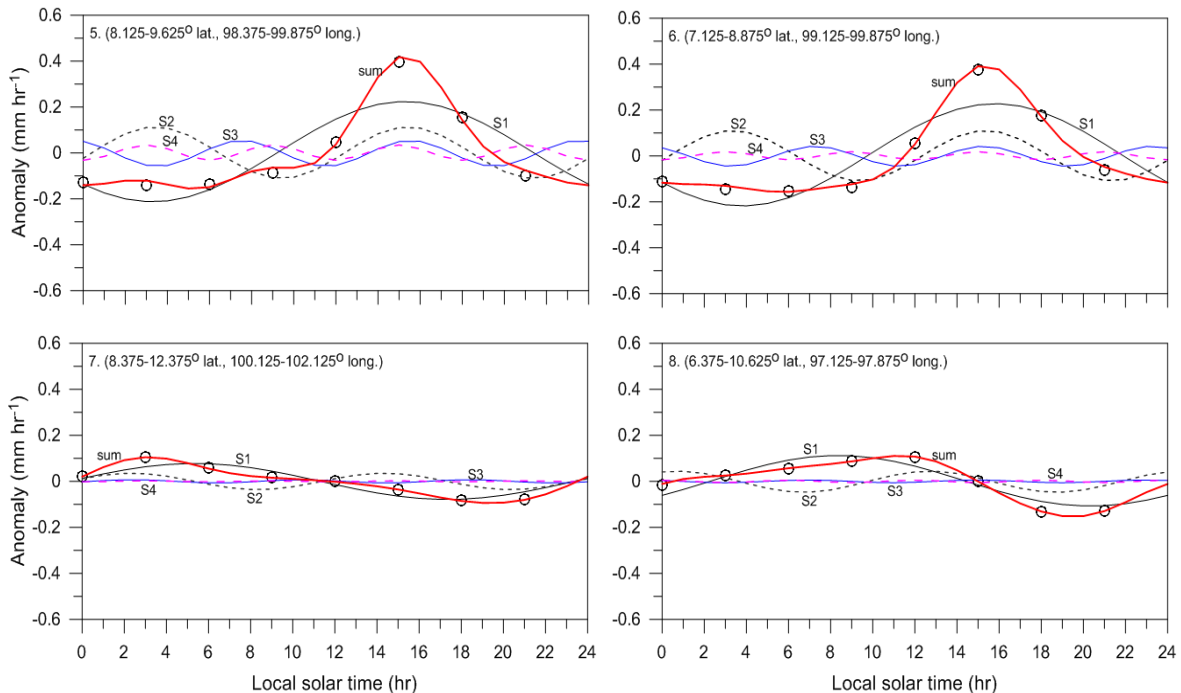
Table 2. Mean second harmonic parameters of sub-daily precipitation variations.

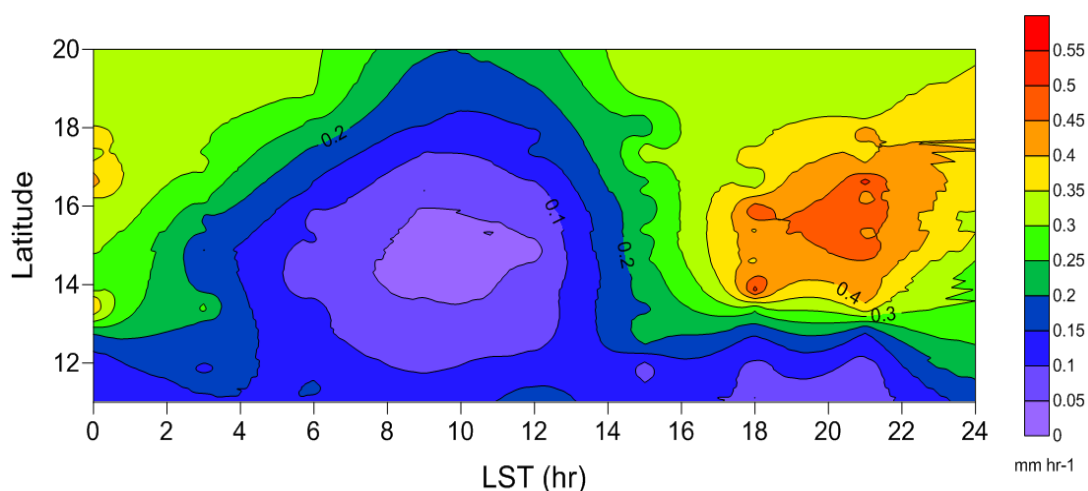| Area	Variance (%)	Amplitude* (%)	Phase (LST)
1	14.9	17.5	4.53
2	13.7	16.5	5.15
3	7.1	22.7	6.14
4	9.0	21.2	4.33
5	18.9	32.1	4.07
6	17.7	32.5	3.22
7	26.5	21.4	2.55
8	11.5	9.8	8.16

*percentage relative to 3-hourly means of precipitation during a rainy season for the period 2000-2009

Figure 4. Climatological mean anomalies of 3-hourly precipitation amount during a rainy season (black open dots), and sub-daily variations estimated by the first (black line), second (black dash line), third (blue line), fourth (magenta dash line) harmonics and sum of first to fourth harmonics (red line) for area 1, 2, 3 and 4, respectively.

Figure 5. Climatological mean anomalies of 3-hourly precipitation amount during a rainy season (black open dots), and sub-daily variations estimated by the first (black line), second (black dash line), third (blue line), fourth (magenta dash line) harmonics and sum of first to fourth harmonics (red line) for area 5,6,7 and 8 respectively.

Figure 6. A LST-latitude plot of climatological means of 3-hourly precipitation amount along 100.375 longitudinal transect.

Averaged amplitudes of sub-daily precipitation amount estimated from the first harmonics for all selected areas ranged from 29.7 to 87.6% of 3-hourly climatological means (Table 1). Results also revealed that relative amplitudes over land areas were stronger than coastal seas (Figures 4 and 5 and Table 1), broadly consistent with the previous analyses of surface and satellite precipitation data demonstrating diurnal variations in tropical and mid-latitude precipitation being larger relative amplitudes over land areas (up to 100% of the daily mean) during the warm season than over oceans [10]. The amplitudes of semi-diurnal cycle ranged from 9.8 to 32.5% (Table 2), and were considerably weaker than the diurnal cycle for all selected areas. By comparison, the semi-diurnal amplitudes in the peninsula (areas 5 and 6) were relatively larger than those in other areas (Figures 4 and 5 and Table 2). Analyzing diurnal variations of precipitation in the warm season over China based on 48-year hourly data from 63 rain gauges during 1954-2001, Yin et al. (2009) [4] found that the semidiurnal amplitudes ranged from 1 to 30% of the daily mean, comparable to what was observed from this study.

Phase of the S1 and S2 can be expressed by the LST when the diurnal and semidiurnal harmonic peaks. The observed S1 peaked in the afternoon [1400-1500 LST] and in the evening (1800-2000 LST) over peninsula and main land, and in the early morning [0500-0900 LST] over coastal seas (Figures 4 and 5 and Table 1). These results are consistent with out-of-phase diurnal patterns generally reported over land and ocean [3, 10, 34]. The S2 phase was, however, similar for both land and coastal seas, to the time of maxima ranging from 0200 to 0800 LST (Table 2). It is worth to note that the diurnal phases identified by harmonic analysis for all selected areas are in good agreement with the principal component coefficient series of the two leading EOFs (Figures 3, 4 and 5 and Tables 1 and 2). The LST-latitude plot of climatological means of 3-hourly precipitation amount along 100.375 longitudinal transect (Figure 1) also shows late afternoon and evening peaks over land (Figure 6), similar to the detected phase of S1 (Table 1). However, obvious maximum of climatological means of 3-hourly precipitation amount was not observed over the Gulf of Thailand along 100.375 longitudinal transect (Figure 6).

4. Conclusions

The spatial patterns of diurnal cycles of precipitation during a rainy season over Thailand and its vicinity were analyzed using 3-hourly, 0.25° TRMM data for the time period 2000-2009 in this study. The EOF and harmonic techniques were found to be a powerful tool to describe diurnal precipitation

variations in the tropical regions where are under strong influence by the Asian summer monsoon. Results revealed that the leading two EOFs and harmonics alone could explain most of the variation of diurnal precipitation (> 90%) over the study domain. The first EOF and harmonic represent the 24-h predominating cycle, which has an afternoon-evening peak and amplitude of 30-88% of the 3-hourly climatological mean. This dominant feature indicates the fundamental land-sea contrast of diurnal precipitation variations with opposite signs observed for the land and coastal sea. It reflects the land-sea difference in the atmospheric response to solar radiation forcing, representing the rise and fall of potential instability forced by the surface heat flux, insolation and long-wave radiative cooling during the day and night. Whereas, the second EOF and harmonic denote the 12-h semidiurnal cycle, with nocturnal and early morning maxima and amplitude of 10-33% of the 3-hourly climatological mean. This secondary sub-daily cycle represents a complementary local variation, and is usually associated with intrinsic mesoscale dynamics of convective systems and its interactions with local thermally induced circulations. The observational evidence obtained here provides a metric to broaden the understanding of local short-term climate and to validate certain parameterizations in numerical models as well as to improve short-term weather forecast accuracy. Apart from its scientific relevance, the results of this study will be useful to the society as well for planning of outdoor activities in different parts of the country. Since the diurnal variations of precipitation are determined by large-scale convective processes as dynamic backgrounds, further analysis should relate the identified diurnal variations to the large-scale atmospheric circulation modes such as Asian Monsoon, Madden-Julian Oscillation (MJO) and El Niño Southern Oscillation (ENSO), and to model simulations. This work may lead to better understanding of mechanisms of precipitation diurnal variations under a recent widening of the tropical belt and an anthropogenically warmed climate.

6. References

[1] Yang G-Y, Slingo J, The diurnal cycle in the tropics, *Mon Weather Rev* 129 (2001) 784-801.

[2] Sorooshian S, Gao X, Hsu K, Maddox RA, Hong Y, Gupta HV, Imam B, Diurnal variability of tropical rainfall retrieved from combined GOES and TRMM satellite information, *J Clim* 15 (2002) 983-1001.

[3] Kikuchi K, Wang B, Diurnal precipitation regimes in the global tropics, *J Clim* 21 (2008) 2680-2696.

[4] Yin S, Chen D, Xie Y, Diurnal variations of precipitation during the warm season over china, *Int J Climatol* 29 (2009) 1154-1170.

[5] Takahashi HG, Fujinami, H, Yasunari T, Matsumoto J, Diurnal rainfall pattern observed by Tropical Rainfall Measuring Mission Precipitation Radar (TRMM-PR) around the Indochina peninsula, *J Geophys Res* 115 (2010) D07109 DOI:10.1029/2009JD012155.

[6] Wallace J, Diurnal variations in precipitation and thunderstorm frequency over the conterminous United States, *Mon Weather Rev* 103 (1975) 406-419.

[7] McGarry MM, Reed RJ, Diurnal variations in convective activity and precipitation during phases II and III of GATE, *Mon Weather Rev* 106 (1978) 101-113.

[8] Albright MD, Recker EE, Reed RJ, Dang R, The diurnal variation of deep convection and inferred precipitation in the central tropical Pacific during January–February 1979, *Mon Weather Rev* 113 (1985) 1663-1680.

[9] Dai A, Giorgi F, Trenberth KE, Observed and model simulated precipitation diurnal cycle over the contiguous United States, *J Geophys Res* 104 (1999) 6377–6402.

[10] Dai A, Lin X, Hsu K-L, The frequency, intensity, and diurnal cycle of precipitation in surface and satellite observations over low- and mid-latitudes, *Clim Dyn* 29 (2007) 727-744.

[11] Dai A, Global precipitation and thunderstorm frequencies. Part II: diurnal variations, *J Clim* 14 (2001) 1112–1128.

[12] Roy SS, Balling RC, Diurnal variations in summer season precipitation in India, *Int J Climatol* 27 (2007) 969-976.

[13] Nesbitt SW, Zipser EJ, The diurnal cycle of rainfall and convective intensity according to three years of TRMM measurements, *J Clim* 16 (2003) 1456-1475.

[14] Yang S, Smith EA, Mechanisms for diurnal variability of global tropical rainfall observed from TRMM, *J Clim* 19 (2006) 5190-5226.

[15] Hsu KL, Gao XG, Sorooshian S, Gupta HV, Precipitation estimation from remotely sensed information using artificial neural networks, *J Appl Meteorol* 36 (1997) 1176-1190.

[16] Sorooshian S, Hsu K-L, Gao X, Gupta HV, Imam B, Braithwaite D, Evaluation of PERSIANN system satellite-based estimates of tropical rainfall, *Bull Am Meteorol Soc* 81 (2000) 2035-2046.

[17] Kidd CK, Kniveton DR, Todd MC, Bellerby TJ, Satellite rainfall estimation using combined passive microwave and infrared algorithms, *J Hydrometeorol* 4 (2003) 1088-1104.

[18] Huffman GJ, Adler RF, Bolvin DT, Gu GJ, Nelkin EJ, Bowman KP, Hong Y, Stocker EF, Wolff DB, The TRMM multisatellite precipitation analysis (TMPA): Quasi-global,

[19] multiyear, combined-sensor precipitation estimates at fine scales, *J Hydrometeorol* 8 (2007) 38-55.

[19] Simpson J, Kummerow C, Tao W-K, Adler R, On the Tropical Rainfall Measuring Mission (TRMM), *Meteorol Atmos Phys* 60 (1996) 19-36.

[20] Kummerow C, Simpson J, Thiele O, Barnes W, Chang ATC, Stocker E, Adler RF, Hou A, Kakar R, Wentz F, Ashcroft P, Kozu T, Hong Y, Okamoto K, Iguchi T, Kuroiwa H, Im E, Haddad Z, Huffman G, Ferrier B, Olson WS, Zipser E, Smith EA, Wilheit TT, North G, Krishnamurti T, Nakamura K, The status of the Tropical Rainfall Measuring Mission (TRMM) after two years in orbit, *J Appl Meteorol* 39 (2000) 1965-1982.

[21] Hirose M, Oki R, Shimizu S, Kachi M, Higashiuwatoko H, Fine scale diurnal rainfall statistics refined from eight years of TRMM PR data, *J Appl Meteor Climatol* 47 (2008) 544-561.

[22] Pribadi A, Wongwises P, Humphries U, Limsakul A, Wangwongchai A, Diurnal rainfall variation over three rainfall regions within Indonesia based on ten years of TRMM data, *J Sus Ene Env* 3 (2012) 81-86.

[23] Angelis CF, McGregor GR, Kidd C, Diurnal cycle of rainfall over the Amazon Basin, *Clim Res* 26 (2004) 139-149.

[24] Basu BK, Diurnal Variation in Precipitation over India during the Summer Monsoon Season: Observed and model predicted, *Mon Weather Rev* 135 (2007) 2155-2167 DOI: 10.1175/MWR3355.1.

[25] Preisendorfer RW, *Principal Component Analysis in Meteorology and Oceanography* (1988) Elsevier, New York, USA.

[26] Emery WJ, Thomson RE, *Data Analysis Methods in Physical Oceanography* (1997) Pergamon Press, New York, USA.

[27] Von Storch H, Zwiers FW, *Statistical Analysis in Climate Research* (1999) Cambridge University Press, Cambridge, UK.

[28] Hannachi A, Jolliffe IT, Stephenson DB, Empirical orthogonal functions and related techniques in atmospheric science: A review, *Int J Climatol* 27 (2007) 1119-1152.

[29] Thompson DWJ, Wallace JM, The Arctic Oscillation signature in the wintertime geopotential height and temperature fields, *Geophys Res Lett* 25 (1998) 1297-1300.

[30] Knutson TR, Weickmann KM, 30–60 day atmospheric oscillations: Composite life cycles of convection and circulation anomalies, *Mon Weather Rev* 115 (1987) 1407-1436.

[31] Teo C-K, Koh T-Y, Lo JC-F, Bhatt BC, Principal component analysis of observed and modeled diurnal rainfall in the Maritime Continent, *J Clim* 24 (2011) 4662-4675 DOI: 10.1175/2011JCLI4047.1.

[32] Chokngamwong R, Chiu LS, Thailand daily rainfall and comparison with TRMM products, *J Hydrometeorol* 9 (2008) 256-266.

[33] Qian JH, Why precipitation is mostly concentrated over islands in the Maritime Continent, *J Atmos Sci* 65 (2008) 1428-1441.

[34] Dai A, Trenberth KE, (2004). The diurnal cycle and its depiction in the community climate system model, *J Clim* 17 (2004) 930-951.